ELSEVIER

Chemical Engineering Journal 66 (1997) 111–121

Chemical Engineering Journal

Diffusivities of organic electrolytes in water

L.A.M. van der Wielen *, M. Zomerdijk, J. Houwers, K.Ch.A.M. Luyben

Department of Biochemical Engineering, Delft University of Technology, Julianalaan 67, 2628 BC Delft, The Netherlands

Received 21 December 1995; accepted 14 July 1996

Abstract

The diffusivities in water of large organic ions such as biomolecules are not readily available. There is a need for adequate measurement and estimation methods. In this work, a rapid method is presented for the determination of diffusivities of ionic species in aqueous systems, based on steady state conductivity measurements. As transient composition gradients are essentially absent in our proposed method, an important source of errors in the form of poorly controlled gradients in thermodynamic non-ideality is eliminated.

Ionic transport is described with the generalized Maxwell–Stefan model, taking friction between solvent and ionic solutes, and between the moving ionic species into account. Ion–water diffusivities could be correlated satisfactorily for a wide range of organic ions, zwitterions and neutral species with the Wilke–Chang relation, and to a lesser extent with a modified Stokes–Einstein relation. Furthermore, the model describes ionic fluxes over a large range of concentrations when corrected for concentration and temperature dependent viscosity effects, by using a modified Stokes–Einstein relation. © 1997 Elsevier Science S.A.

Keywords: Diffusivity; Organic electrolytes

1. Introduction

Knowledge of diffusivities of (bio-)organic electrolytic (and non-electrolytic) molecules in the liquid phase is important for the prediction of mass transfer in chemical and biochemical unit operations. For analytic separation methods such as capillary electrophoresis, knowledge of diffusivities might assist in the rapid optimization of the analytic separation and in the identification of species. Problems associated with the determination of diffusivities of (bio-)organic electrolytes are the following.

1. Most experimental methods to determine diffusivities require skilled experimeters, which reduces their utility as a routine technique.
2. There is an effect of electrostatic interaction with the counter-ion or with other charged solutes on the transport of the bio-organic ions [1,2].
3. The effect of the composition and temperature of the aqueous mixture on the transport of the bio-organic ions is often unknown.
4. A good correlation of diffusivities in dilute, aqueous concentrations with molecular properties is required [3].

* Corresponding author. Tel: +31 15 2782361; fax: +31 15 2782355; e-mail: Vanderwielen@stm.tudelft.nl

PII S1385-8947(96)03167-3

1.1. Determination of diffusivities

Wong and Hayduk [4] and Rutten [3] have recently reviewed techniques for measuring ('free') liquid diffusion coefficients. Newman [5] indicated the possibility of estimating infinite dilution diffusivities of ions from equivalent conductances. Table 1 gives an overview of some established experimental techniques.

The Taylor method is generally preferred because of its speed (30–60 min per determination), good accuracy which is usually within 2% [3], and its applicability for both ionic and non-ionic species. However, setting up this method requires skilled experimenters, though it appears possible to automate it. This generally improves the accuracy. Both interferometry and the diaphragm cell method are relatively time consuming.

A problem for these three transient methods, which is not obvious at first sight, is that transient gradients in composition arise. The corresponding transient gradients in thermodynamic non-ideality can significantly influence the measurements. Although a skilled experimenter may obtain reproducible results, the accuracy of the experimental result depends on the control of the sharpness of the composition gradient. Fickian diffusivities of ethanol in the system ethanol–water as a function of composition [6] may serve as an example, although the system is non-ionic. The diffusivities

Table 1
Overview of experimental techniques for the determination of diffusion coefficients

Technique	Mode	Approximateexperimental time	Neutral species	Calibration required	Experimental skills
Diaphragm cell	Steady/transient	day	Yes	Yes	Medium
Interferometry	Transient	hour	Yes	No	High
Taylor dispersion	Transient	minute–hour	Yes	No	High
Electric conductance	Steady	second	No	No	Low

vary by a factor of 3 owing to the thermodynamic non-ideality at changing composition, as is shown in Fig. 1 [7]. Similar strong concentration dependences are mentioned by Newman [5] and Reid et al. [8], especially for electrolyte systems at low concentrations.

The last method in Table 1, the electric conductance method, is based on the measurement of ionic transport, in the form of the equivalent conductances, under the influence of an electrical field over a homogeneous solution between two electrodes. Hence, possible effects of gradients in liquid composition are eliminated in this method. Another advantage is the very short time required per determination, typically seconds, and the relatively low skill requirements. In addition, this method seems suited for automation. A disadvantage, however, is the limitation to ionic species only.

1.2. The effects of mixture composition

It has been shown that the transport of ions in solutions is strongly composition dependent [5,8]. This effect becomes apparent at very low concentrations (below 1 mol m^{-3}) owing to the strong, long range electrostatic interactions between the ions. The long range effect was illustrated beautifully by Cadman et al. [9] for the diffusion of the cationic protein lysozyme in the presence of its multiple Cl^- counterions. Here, the relatively large lysozyme ion was accelerated by the small, mobile chloride ions, which results in abnormally high diffusion coefficients for the neutral protein salt (lysozyme + Cl^- ions). Alternative examples were presented by Krishna [1].

For high concentrations of electrolytes, short range interactions of solvent and solutes should also be accounted for.

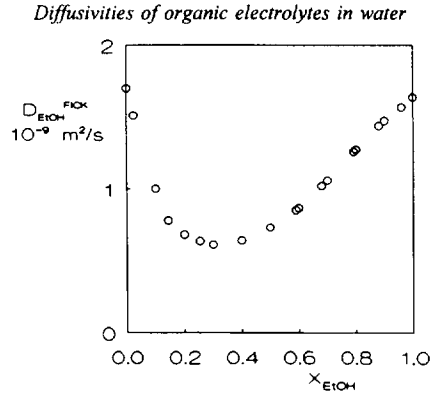

Fig. 1. Fickian diffusivity of ethanol in ethanol–water for various compositions at 298 K. Data from Tyn and Calus [6].

These interactions are reflected in the decreased diffusivities and also through the increased viscosity of the solution. Unfortunately, reliable transport data for binary and multicomponent electrolyte solutions at high concentrations are particularly scarce [5]. So far, the relation between decreased diffusivities, increased short range interactions and increased solution viscosity has only been discussed qualitatively [5].

The occurrence of long range electrostatic and short range interactions at increased electrolyte concentrations has restricted earlier applications of the electric conductance method to the determination of infinite dilution diffusivities only. In this work, we seek to account for these effects, so as to extend the range of applicability of the electric conductance method. Anticipating Section 2 and Section 4, the long range electrostatic interactions are accounted for using of the Maxwell–Stefan model, whereas the effect of short range interactions is incorporated using a viscosity correction.

1.3. Predictive correlations

Notwithstanding the importance of the effects discussed in the preceding section, the solute–solvent (here the ion–water) interaction dominates the overall friction. Hence, reliable prediction of this solvent–solute interaction, evident in the diffusivity, is very valuable. A number of these correlations is known [3], which all have the friction model of Stokes and Einstein as the starting point. The Stokes–Einstein model relates the macroscopic model for motion of an incompressible sphere in a viscous fluid to molecular diffusion phenomena. The resulting Stokes–Einstein equation expresses the diffusivity in terms of the molecular volume of the solute i via its characteristic radius R_i and the viscosity of the solvent j:

$$Đ_{ij}(x_i \to 0) = \frac{kT}{n_{SE}\pi\eta_j R_i} \tag{1}$$

The Stokes–Einstein parameter n_{SE}^0 has reported values of 4 to 6. The radii are computed from the Van der Waals or critical molar volumes by regarding the molecules as spherical. Rutten [3] has modified this approach by evaluating the relation of the ratio of solute and solvent radius on the observed Stokes–Einstein parameter n_{SE}. Also the effect of solute–solute, solvent–solvent and solute–solvent clusters by association mechanisms such as hydrogen bonding was analysed. Rutten [3] classified solute–solvent combinations depending on their polarity and their tendency to aggregate.

The result was a modified Stokes–Einstein relation for infinite dilution, solute–solvent diffusivities:

$$D_{ij}^{SE} = D_{ij}(x_i \to 0) = \frac{kT}{n_{SE}^0 \pi \eta_j R_i}\left[\frac{R_j}{R_i}\right] \quad (2)$$

while obtaining different n_{SE}^0 values for each of the categories. For sets of diffusivities in the same solvent, this yielded the following dependence on the molecular volume:

$$Đ_{ij}(x_i \to 0) \sim V_i^{-2/3} \quad (3)$$

This general form has been the starting point for many other correlations. Molecular volumes are those at the boiling point, which have been obtained from the well known group contribution method of LeBas (in [8]). Critical volumes, Van der Waals volumes and molar volumes at the normal boiling point are strongly interrelated, and for reasons of coherence with the following section, we have used the latter. One of the earliest and most famous (empirical) correlations is that of Wilke and Chang [10], which reads as follows:

$$Đ_{ij}^{WC} = Đ_{ij}(x_i \to 0) = 7.14 \times 10^{-8} \frac{\sqrt{\chi M_j}\, T}{\eta_j V_i^{0.6}} \quad (4)$$

M_j is the molar mass of the solvent in g mol^{-1}, η_j is the solvent viscosity in cP, and V_i is the molar (Le Bas) volume of the solute at its normal boiling point. The parameter χ indicates the degree of association of the solvent. In the original correlation, its value was 2.6 for water. Hayduk and Laudie [11] reported a value of 2.26 to be optimal. It has been noticed [3] that the original correlations are usually not too accurate for polar solutes in polar solvents such as water. Therefore, the usefulness of these correlations for predicting ion–water interactions should be evaluated.

1.4. Aim of this paper

In this work, we summarize a systematic methodology for measuring, evaluating and predicting ionic transport in aqueous solution. Firstly, we present the theoretical framework for describing ionic transport in aqueous solution. The framework is based on the Generalized Maxwell–Stefan equations [7] and incorporates the effects of composition through long range (electrostatic) and short range interactions. Subsequently, the experimental method, based on measurement of electric conductance, is outlined and applied to newly obtained and known literature data. This method is used to determine the diffusivities of organic electrolytes such as carboxylic acids and β-lactam antibiotics. In addition, the usefulness of some correlations for predicting diffusivities of electrolytic components is tested for a wide range of organic electrolytes (and non-electrolytes).

2. Modelling

2.1. Electric conductance

Thus, diffusivities can be obtained directly from measuring the electric conductivity. In the following section, we outline the relation between conductivity, transport of ions (ionic fluxes) and the diffusivities of ions. As conductivities can be measured directly, we start the development of the theoretical framework at this end.

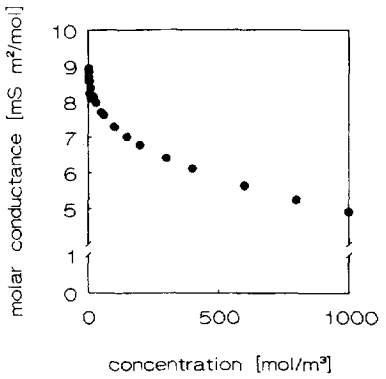

Fig. 2. Ionic equivalent conductances of an aqueous sodium acetate solution. Data from Landolt–Börnstein [12].

Conductivities are not readily found in the literature, but ionic equivalent conductances λ are tabulated at infinite dilution and as a function of the concentration [5,8,12]. The conductivity κ of an electrolyte solution can be expressed in terms of ionic equivalent (or molar) conductances λ_i;

$$\kappa = \sum_j |z_j| \lambda_j c_j \quad (5)$$

Already at very low concentrations, ion–ion friction is important. This is demonstrated in Fig. 2, giving the molar conductance of sodium acetate at 298 K obtained from [12] as an example. The ionic equivalent conductances are strong, declining functions of increasing solute concentration.

The conductivity κ is related via the known external electric field (and its electric potential gradient $\nabla\phi$) to the measured current density, according to:

$$I = -\kappa \nabla \phi \quad (6)$$

The current density I due to electrolyte transport can be expressed in terms of fluxes of the individual electrolytes, as follows:

$$I = \sum_j z_j J_j \quad (7)$$

In the following section, a thermodynamically rigorous relation between ionic fluxes, electric potential and the wanted diffusivities is provided.

2.2. Transport of electrolytes in aqueous solution

The generalized Maxwell–Stefan equation relates the driving forces for transport to the encountered frictional resistance [7]. In the case of transport of electrolytes in aqueous solution, the driving forces are usually gradients in chemical composition and in electric potential. A moving ion encounters frictional resistance from water, and at higher concentration, from other solutes. Transport of a key component i in a

multi-component system therefore can be described by the following flux relation:

$$x_i\nabla\mu_i + x_i z_i\frac{F}{RT}\nabla\phi = \frac{x_i J_w - x_w J_i}{c\mathcal{D}_{iw}} + \sum_{j\neq w}\frac{x_i J_j - x_j J_i}{c\mathcal{D}_{ij}} \quad (8)$$

with x_i being the mole fraction, c the total concentration, J_i the molecular flux and $\mathcal{D}_{ij}$ the Maxwell–Stefan diffusion coefficient for friction between species i and j. The terms in the left-hand side of Eq. (8) are relevant driving forces for electrolyte transport in the absence of strong centrifugal or pressure fields. The first term is the contribution of the composition gradient to the overall driving force. The second term presents the influence of an external or diffusion induced electric potential gradient on the driving force. The terms at the right-hand side of Eq. (8) are the frictional forces due to relative motion of the key component i with water (w) and other solutes (j).

Conductance of electrolyte solutions does not involve composition gradients but the electrolyte transport is induced by electric forces only. The composition of the solution between the electrodes is homogeneous. Therefore, the working form of Eq. (8) is

$$x_i z_i\frac{F}{RT}\nabla\phi = -\left[\frac{J_i}{c\mathcal{D}_{iw}} + \sum_j\frac{x_i J_j - x_j J_i}{c\mathcal{D}_{ij}}\right] \quad (9)$$

2.3. Additional relations

Additional relations are required to complete the description of electrolyte transport during electric conductance. An obvious condition is the requirement of electroneutrality. The bootstrap relation [7] in stagnant and not too concentrated solutions, is a negligible water flux ($J_w = 0$).

A satisfactory empirical relation for cation–anion diffusivity has been reported [7]. These authors have evaluated conductivity data of binary inorganic salts over a broad concentration range and obtained the following expression for the frictional interaction between ionic species:

$$\mathcal{D}_{\pm} = 4.8\times10^8\mathcal{D}^{\infty}_{+w}\mathcal{D}^{\infty}_{-w}\frac{I_x^{0.55}}{|z_+z_-|^{1.85}} \quad (10)$$

I_x is the mole fraction based ionic strength of the electrolyte solution. The solvent–ion interactions were originally expressed in the corresponding infinite dilution (Fickian) diffusivities $\mathcal{D}^{\infty}_{+w}\mathcal{D}^{\infty}_{-w}$. These were assumed to be constant for the range of validity of this relation. Also Newman [5] showed a similar square-root-of-concentration dependence for the ion–ion interaction and reasonably constant solvent–ion interaction coefficients. More recently, Kraaijeveld and Wesselingh [13] demonstrated that this is usually valid for concentrations below 1 M. As this ion–ion interaction occurs already at very low concentrations, it will be caused to a large extent by long range electrostatic interactions and therefore will be rather insensitive to the exact chemical nature of the interacting components. In this work, we have used Eq. (10) in its original form.

2.4. Effect of composition and temperature on diffusivities

The Stokes–Einstein model and the correlation of Wilke and Chang indicate a strong dependence of the solute diffusivity on the viscosity of the solvent. The solvent viscosity may change owing to variation in temperature and overall composition. As mentioned before, molecular interactions (expressed as thermodynamic non-ideality) and viscosity are interrelated, but very few experimental correlations exist. For the bio-organic species of interest, the thermodynamic data are practically absent or not easily accessible or measurable, whereas viscosity data are more easily available or measured. Therefore, we have incorporated in this work a lumped dependence of the solute diffusivity on solvent viscosity, according to the modified Stokes–Einstein relation of Versteeg and van Swaaij [14], which was derived for Fickian diffusivities:

$$\frac{D_{ref}}{D} = \left(\frac{\eta}{\eta_{ref}}\right)^{0.6} \quad (11)$$

Hence, composition and temperature dependences of the diffusivities are implicitly corrected for by the overall viscosity correction. This relation was proved to be valid for Fickian diffusivities in aqueous alkanol–amine solutions for a broad range of concentrations (0–4000 mol m^{-3} [15]). Increasing the solute concentration violates the previous assumption of a zero water flux. A non-zero water flux may be the actual reason of a decrease in the diffusivities with increasing concentrations. However, this is difficult to validate experimentally whereas a viscosity correction using Eq. (11) is a straigtforward procedure.

2.5. Parameter sensitivity

Experimental values of infinite dilution diffusivities of organic ions as large as β-lactam antibiotics are in the range of 0.1×10^{-9} to 2×10^{-9} m^2 s^{-1} [16,17]. To investigate the sensitivity of conductivity measurements for the diffusivities at infinite dilution, we have performed some simulations using the model described in the previous sections. Simulations have been performed with a cation–water diffusivity of 2×10^{-9} m^2 s^{-1}. This could stand for potassium as the common cation, which has an infinite dilution diffusivity of 1.957×10^{-9} m^2 s^{-1} at 298 K. Simulations for the molar conductance as a function of the electrolyte concentration have been performed for the usual concentration range of 1–100 mol m^{-3}. The results are shown in Fig. 3. A minimum accuracy of approximately 0.1×10^{-4}–1.0×10^{-4} S m^2 mol^{-1} is required to reduce the measurement error to about 1%. This accuracy is easily accomplished with commercially available equipment for measuring electric conductivity.

3. Experimental details

The potassium salt of penicillin G was a gift of Gist-brocades nv and was 99.2% pure. All other components were of

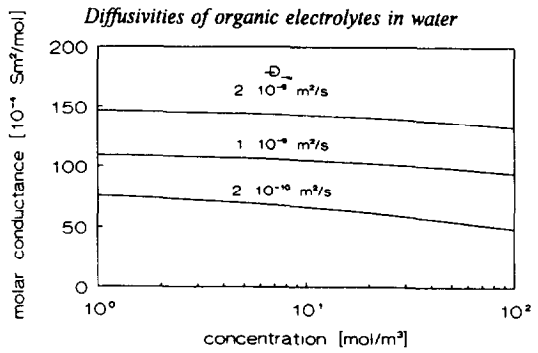

Fig. 3. Computed molar conductances of solutions with a common cation with $\mathcal{D}_{+w} = 2 \times 10^{-9}$ m^2 s^{-1} for anions with different diffusivities $\mathcal{D}_{-w}$.

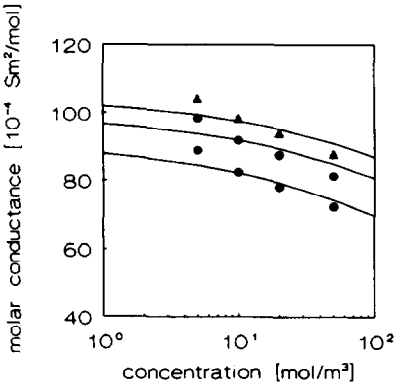

Fig. 4. Molar conductances of potassium salts of 6-aminopenicillanic acid (○), phenylacetate (●), and penicillin G (■) at 298 K. The curves are calculated from Eq. (9) and Eq. (10) using the $\mathcal{D}_{-w}$ given in the text.

analytical grade (obtained from Fluka) and weighed amounts were dissolved in a known mass of deionized water (checked by electrical conductivity). The water was prepared with a Milli-Q water system (Millipore, France). Since the components are weak electrolytes, they were converted into their potassium form by the addition of a known mass of analytically pure KOH solution from Merck. The pH was adjusted to neutral (pH 7), which is well above the pK_a value of the compounds. This pH also reduces the unwanted influence of protons or hydroxide ions on the conductivity. The masses were determined on a Mettler Toledo balance, model AB204 (Mettler, Switzerland) with a resolution of 0.0001 g. The error in the concentration of the final solution is estimated to be smaller than 2%.

Conductivities of the components were obtained with a Consort K610 conductivity meter and a Philips flow-through conductivity electrode in a 100 ml jacketed vessel with temperature control. The temperature was maintained at 298 K during the experiments. The conductivity electrode had a cell constant of 0.734 cm^{-1}. Conductivities have been measured with a resolution of 0.1 mS for 5–50 mol m^{-3} solutions of phenylacetate, 6-aminopenicillanate acid and benzylpenicillanate at pH 7 and 298 K. The error in the conductivity measurement was smaller than 1%. The common counter-ion K^+ was used for calibration purposes, and KCl was used as a reference component for the the conductivity measurements. The KCl was also analytically pure and obtained from Merck.

The composition dependence of the conductivity of KCl and the diffusion coefficients of the individual ions have been reported extensively in the literature. The concentration dependence of viscosities has been taken from the literature [18], as well as the molar conductances of 23 carboxylic acids [12].

4. Results

4.1. Experimental results

The experimental procedure has been checked using conductivity measurements for KCl solutions at 298 K over the concentration range 1–1000 mol m^{-3}. The molar conductances, which were calculated by dividing the conductivity through the actual concentration, were compared with molar conductances obtained from Landolt–Börnstein ([12], Series S4, C6 and C4b). The average deviation of our data and those from Landolt–Börnstein was 2%, which is within the estimated error of the concentration.

Following the same procedure, experimental molar conductances of solutions of the potassium salts of 6-aminopenicillanic acid (APA), phenylacetic acid and benzylpenicillin (Pen G) were determined at 298 K. These are shown as the symbols in Fig. 4. It was assumed that these data had the same average deviation in the molar conductance as was observed for KCl.

Molar conductances for the anions of the carboxylic acids shown in Table 2 were taken from the literature. Molar conductances were taken from the compilation by Landolt–Börnstein [12], unless indicated differently in Table 2.

4.2. Interpretation of the data

The following procedure was used to estimate the solute–water diffusivities in electrolyte solutions. The fluxes of ions in an electrolyte solution for a given electric potential gradient are calculated using Eq. (9) for both cation and anion of the salt for a given set of Maxwell–Stefan diffusivities. The ion–water diffusivity for the cation is fixed and that of the anion is estimated. The composition dependent ion–ion diffusivity is calculated using Eq. (10). The resulting current density and molar conductance are calculated from the fluxes using Eq. (7), Eq. (6) and Eq. (5) respectively. The calculated molar conductances are then compared with the experimental values. The sum of the squared differences was minimized by varying the anion–water diffusivity using the Simplex method.

4.3. Resulting diffusivities

4.3.1. Data from this work

Following the above procedure and setting the infinite dilution diffusivity of K^+ at its literature value (1.957×10^{-9} m^2 s^{-1}), we found a value for the Cl^- anion of 1.97×10^{-9}

Table 2
Overview of diffusion coefficients in 10^{-9} m^2 s^{-1} of organic acids and β-lactam antibiotics in water at 298 K

	V_{LeBas} 10^{-6} m^3 mol^{-1}	Eq. (4) $\chi=2.9$	Eq. (2) $n_{SE}^0=2.17$	Neutral	Ionic Na^+	Ionic K^+	Other cations	Infinite dilution
Carboxylic acids								
Formiate	46.2	1.52	1.70	1.52	1.43	1.45	1.46 [a]	1.452
Acetate	64.7	1.26	1.36	1.19	1.12	1.03	1.09 [a]	1.095
Propanoate	86.9	1.06	1.11	1.01	0.937	0.953	0.954 [a]	0.953
Butanoate (butyrate)	109.1	0.92	0.96	0.918	0.849	0.847	0.935 [a]	0.831
Pentanoate (valerate)	131.3	0.82	0.85	0.817			0.890 [a]	
Hexanoate (caproate)	153.5	0.75	0.76	0.784			0.810 [a]	
Dodecanoate (laurate)	286.7	0.52	0.50		0.63			
Lactate	86.9	1.06	1.12			1.44		
Citrate	186.7	0.67	0.67		0.661			0.652
Tartrate	136.8	0.80	0.82					
Oxalate	77.6	1.13	1.20		0.945	0.988		1.004
Malonate	99.8	0.97	1.02		0.87			0.936
Succinate	122	0.86	0.89	0.862			0.812 [a]	0.807
Glutarate	144.2	0.78	0.80	0.787	0.771		0.758 [a]	0.753
Adipate	166.4	0.72	0.72	0.736	0.703		0.705 [a]	0.699
Fumarate	114.6	0.89	0.93					
Benzoate	146.1	0.77	0.79		0.845	0.864		0.870
Phenylacetate	168.3	0.69	0.70			0.85 [b]		0.866
Phtalate	181.2	0.68	0.68		0.739	0.739		
Salicylate	153.5	0.75	0.76					
Antibiotics								
Benzylpenicillin	395.3	0.43	0.41			0.49 [b]		
6-Aminopenicillinate	242.3	0.57	0.56			0.71 [b]		
Amoxicillin	405.8	0.42	0.40	0.30 [c]				
Ampicillin	398.4	0.42	0.40	0.37 [c] 0.458 [d]				
Epicillin	420.8	0.41	0.39	0.38 [c]				
Cyclacillin	413.4	0.41	0.39	0.37 [c]				
Cephadrin	373.1	0.44	0.42	0.27 [c]				
Cephalexin	380.7	0.44	0.42	0.26 [c]				
Cephaloglycin	443.3	0.40	0.38	0.28 [c]				

Data for zwitterionic and neutral species were largely compiled by Hayduk and Laudie [11], those of ionic species were computed from conductivity data from Landolt–Börnstein [12] except for [a]Albery et al. [19], [b]this work, [c]Tsuji et al. [16,17], recalculated from 310 K data using Eq. (11), [d]Padfield and Kellaway [20].

$m^2\ s^{-1}$. This value is in close agreement with values indicated in the literature ($2.032 \times 10^{-9}\ m^2\ s^{-1}$ [5]).

Fitted values for the Maxwell–Stefan solute–solvent diffusivities using the same procedure were $0.85 \times 10^{-9}\ m^2\ s^{-1}$ for the anions of phenylacetic acid, $0.71 \times 10^{-9}\ m^2\ s^{-1}$ for 6-aminopenicillanic acid and $0.49 \times 10^{-9}\ m^2\ s^{-1}$ for benzylpenicillin. The curves drawn in Fig. 4 are simulations with the Maxwell–Stefan model (Eq. (9)) using fitted solute–solvent diffusivities and Eq. (10) for the ion–ion interaction. Because the concentrations of the solutes do not exceed 50 mol m^{-3}, the influence of a possible viscosity increase was neglected for these calculations.

The simulations and measured conductivities of potassium phenylacetate, 6-aminopenicillanate and benzylpenicillinate deviated systematically at low concentrations. The deviation was not observed for the KCl solutions. This can hardly be a viscosity effect as the deviation has its largest value at lowest concentrations. It might be due to a deviation of the diffusivity of K^+ with organic ions under our conditions from its value in aqueous Cl^- solutions, in combination with the possibly limited accuracy of Eq. (10).

4.3.2. Literature data for diluted systems

Maxwell–Stefan diffusivities $Đ_{-w}$ of the carboxylates in Table 2 are also obtained by fitting Eq. (9) and Eq. (10) to their molar conductances from [12] as a function of concentration. The $Đ_{+w}$ data for the (inorganic) counterions of the carboxylates are assumed to be equal to the infinite dilution value, as reported in [5]. In general, a reasonable agreement was observed for one single value of the $Đ_{-w}$ coefficient for concentrations below 100 mol m^{-3}.

4.3.3. Higher concentrations

However, molar conductances at higher concentrations (greater than 100 mol m^{-3}) were overestimated when using Maxwell–Stefan diffusivities obtained at lower concentrations. A typical example, in this case for sodium acetate, is shown in Fig. 5, which illustrates this phenomenon.

Hence, we have corrected the solvent–solute diffusivities at the actual composition for the increased viscosities at higher electrolyte concentrations with the modified Stokes–Einstein Eq. (11). Fig. 6 shows the ratios of actual viscosity and viscosity at infinite dilution of the selected sodium salts (acetate, oxalate and citrate [18]). The increase in viscosity is negligible for solute concentrations below 100 mol m^{-3} for monovalent and bivalent anions (below 5%), and still relatively small (below 10%) for trivalent species. The viscosity was described as a function of the concentration by fitting a polynomial relation through the data, obtained from [18]. The improved correlation of the experimental data for the case of sodium acetate is shown as the solid curve in Fig. 5.

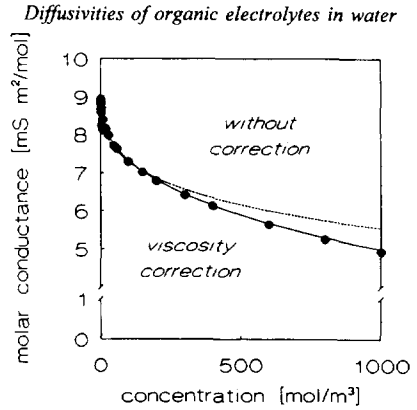

Fig. 5. Molar conductance as function of concentration for aqueous solutions of sodium acetate at 298 K. Data from Landolt–Börnstein [12]; curves simulated with Eq. (9) and Eq. (10).

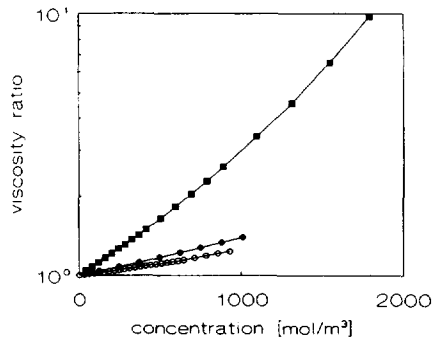

Fig. 6. Ratio of viscosity to the viscosity in the absence of sodium salts of acetate (●), oxalate (○) and citrate (■). Data from Weast [18].

The resulting Maxwell–Stefan ion–water diffusivities from the potassium, sodium or calcium salts of 23 carboxylic acids are derived from original experiments or from literature data and are compiled in Table 2. From various other literature sources, the diffusivities of the corresponding neutral acids and infinite dilution ionic diffusivities have been obtained. Literature diffusion data for these species and for β-lactam antibiotics, as well as literature sources, are given in Table 2 as well.

5. Discussion

5.1. Are Maxwell–Stefan and infinite dilution diffusivities identical?

A comparison of the values of the Maxwell–Stefan solvent–anion coefficient $Đ_{-w}$ and those from infinite dilution data suggest that these are identical. Fig. 7 is a parity plot of Maxwell–Stefan diffusivity and the infinite dilution diffusivity. This statement is of course consistent with the physical 'picture' that the infinite dilution situation is largely determined by solute–solvent interaction. In fact, this observation confirms the empirical relation for the Maxwell–Stefan ion–ion interaction coefficient (Eq. (10) [7]). The relation for ion–ion interaction was originally obtained for inorganic electrolytes, but is shown to be valid for organic electrolyte systems as well. This is in agreement with the Debye–Hückel-like long distance electrostatic nature of the interionic friction, which should be largely independent of the chemical character of the ionic species. However, it is expected that at

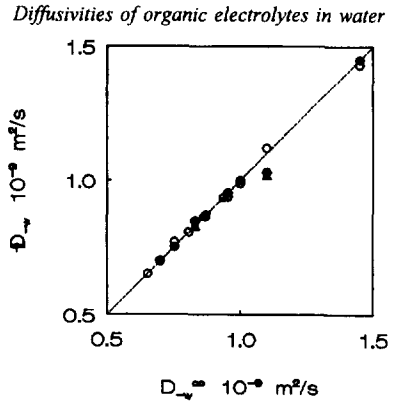

Fig. 7. Parity plot of the infinite dilution and Maxwell–Stefan diffusivities of carboxylic acids. Values from Table 2 and various counter-ions: Na^+ (○), K^+ (●) and other (▲).

very high electrolyte concentrations (5–10 kmol m^{-3}) neither this long distance interaction force nor the Stokes–Einstein viscosity correction will be able to predict accurately ionic transport.

5.2. Are diffusivities of ionic and neutral forms of a weak electrolyte equal?

Another point of interest is the influence of the absence or presence of an electric charge on an organic electrolyte on its mobility. See Fig. 8 for a comparison of infinite dilution (Fickian) diffusivities of neutral and ionic forms of carboxylic acids at 298 K. Albery et al. [19] have investigated 13 different monovalent and divalent carboxylic acids with respect to this question. They concluded that monovalent ions are on average as mobile as the neutral species whereas bivalent ions tend to be some 5% less mobile than their neutral counterparts. The smaller diffusivity was attributed to a tight ion–water binding and hence a larger solvation volume. Our findings show slightly smaller diffusivities for the monovalent ionic form. No data for bivalent ions and the corresponding neutral forms are available to add to Albery's conclusion.

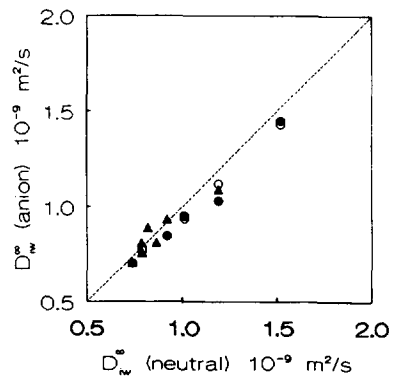

Fig. 8. Parity plot of the diffusivities of neutral and ionic forms of carboxylic acids. Values from Table 2 and various counter-ions: Na^+ (○), K^+ (●) and other (▲).

5.3. Comparison with predictive correlations

The observations made in the preceding section justify the prediction of electrolyte transport from (Fickian) diffusion coefficients at infinite dilution, even at fairly high concentrations. For comparison, infinite dilution diffusivities of other neutral or zwitterionic organic species such as amino acids, peptides, alkanol amines (Table 3), alcohols and carbohydrates (Table 4), have also been compiled.

Hence, we have estimated the Stokes–Einstein parameter n_{SE}^0 by fitting Eq. (2) to the experimental diffusivities for neutral, zwitterionic and ionic species from Tables 2–4. Molecular volumes are estimated from the group contribution method of LeBas [23]. Fig. 9 shows a parity plot of experimental diffusivities and those obtained from the modified Stokes–Einstein relation for an optimal value for n_{SE}^0 of 2.17 with an average deviation of 7.3%. Predicted and experimental values are in good agreement, but have a slight systematic

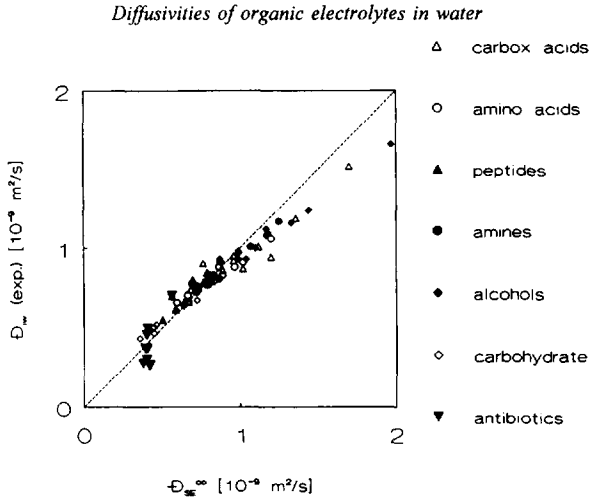

Fig. 9. Parity plot of experimental diffusivities from Tables 2–4 and those calculated from the Stokes–Einstein relation with $n_{SE}^0 = 2.17$.

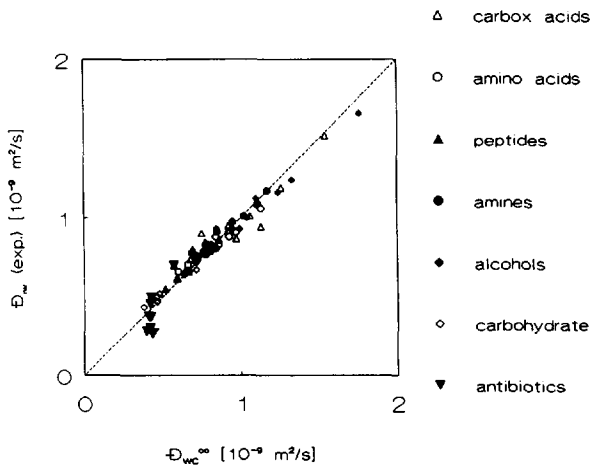

Fig. 10. Parity plot of experimental diffusivities from Tables 2–4 and those predicted with the Wilke and Chang relation with $\chi = 2.9$.

Table 3
Overview of diffusion coefficients in 10^{-9} m^2 s^{-1} of amino acids, peptides and alkanol amines in water at 298 K

	V_{LeBas} 10^{-6} m^3 mol^{-1}	Eq. (4) $\chi=2.9$	Eq. (2) $n_{SE}^0=2.17$	Neutral orzwitterion
Amino acids				
Glycine	78	1.13	1.20	1.06
Alanine	100	0.97	1.02	0.91
Serine	108	0.93	0.97	0.88
Aminobutyrate	122	0.86	0.89	0.83
Valine	145	0.78	0.79	0.77
Leucine	167	0.71	0.72	0.73
Proline	127	0.84	0.87	0.88
Hydroxy-proline	135	0.81	0.83	0.83
Histidine	168	0.71	0.72	0.73
Phenylalanine	189	0.66	0.66	0.705
Tryptophan	223	0.60	0.60	0.66
Threonine	134	0.82	0.83	0.80
Norvaline	145	0.78	0.79	0.77
Norleucin	166	0.71	0.72	0.72
Asparagine	141	0.79	0.81	0.83
Glutamine	165	0.72	0.73	0.76
Amino-benzoate	144	0.78	0.80	0.84
Peptides				
Diglycine	138	0.80	0.82	0.79
Triglycine	198	0.64	0.64	0.67
Glycyl-leucine	227	0.59	0.59	0.62
Leucyl-glycine	227	0.59	0.59	0.61
Leucyl-glycyl-glycine	287	0.52	0.80	0.55
Alkanol amines				
Monoethanolamine	73	1.17	1.25	1.17 [a]
Diethanolamine	127	0.84	0.87	0.81 [a]
Triethanolamine	179	0.69	0.69	0.78 [a]
Methyldiethanolamine	149	0.76	0.78	0.79 [a]
Monoisopropylamine	92	1.02	1.08	1.01 [a]
Diisopropanolamine	164	0.72	0.73	0.74 [a]
Diglycolamine	125	0.85	0.87	0.91 [a]
Ethyldiamine	80	1.11	1.18	1.09 [a]

Data for zwitterionic and neutral species were largely compiled by Hayduk and Laudie [11]. Data for alkanol amines[a] were obtained from Hikita et al. [21], Versteeg and van Swaaij [14] and Snijder [15].

deviation. This may be attributed to a slightly too high value of the exponent of the molecular volume ($-2/3$), which indicates the importance of friction at the molecular surface.

Diffusivities of the larger semi-synthetic antibiotics, which were obtained from the work of Tsuji et al. [16,17], are largely overestimated by the Stokes–Einstein relation. These diffusivities have been obtained by the steady state diaphragm method at 310 K. We have recalculated these data to 298 K using Eq. (11). However, the error which was introduced by this procedure is smaller than 5% and cannot explain the large deviation of predicted and experimental diffusivity. A discrepancy between the true molecular dimensions and those estimated from LeBas' method could be the cause of this deviation. A closer inspection of the three-dimensional arrangement of the atoms in these semi-synthetic antibiotics can be made from crystallographic data from Crowfoot et al. [23] and Flynn [24]. Although extrapolation of the solid phase dimensions to solution behaviour is highly speculative, it was observed that some molecular bonds are not flexibl e enough to support the assumption of a spherical solute. Consequently, the molecular structure is more 'open' and the relevant dimensions for friction with water are underestimated. It has been demonstrated that characteristic dimensions which reflect more the actual size of a species such as the radius of gyration are better suited for correlating diffusivities of these large species [25].

The Wilke and Chang correlation, Eq. (4), is also based on the Stokes and Einstein friction model. The parameter χ indicates the degree of association of the solvent. In the original correlation, its value was 2.6. Hayduk and Laudie [11] reported a value of 2.26 to be optimal, but for the data set of Table 3, the value of 2.9 gave the best fit (average deviation 5.5%). The better overall prediction of this relation is due to its slightly lower exponent for the molecular volume (0.6 instead of $-2/3$). Fig. 10 is a parity plot of experimental diffusivities and those predicted with the Wilke and Chang equation. Again the data for semi-synthetic antibiotics are overestimated.

Table 4
Overview of diffusion coefficients in 10^{-9} m^2 s^{-1} of alcohols and carbohydrates in water at 298 K

	V_{LeBas} 10^{-6} m^3 mol^{-1}	Eq. (4) $\chi=2.9$	Eq. (2) $n^0_{SE}=2.17$	Neutral
Alcohols				
Methanol	37	1.76	1.97	1.66
Ethanol	59	1.33	1.44	1.24
1-Propanol	81	1.10	1.17	1.08
2-Propanol	81	1.10	1.17	1.12
1-Butanol	104	0.95	0.99	0.93
2-Butanol	104	0.95	0.99	0.98
Benzylalcohol	126	0.84	0.87	0.93
Ethyleneglycol	67	1.24	1.33	1.16
Tri-ethylene glycol	170	0.71	0.71	0.76
Propylene glycol	89	1.04	1.10	1.00
Glycerol	96	0.99	1.04	0.93
Ethane-hexanediol	200	0.64	0.64	0.64
Carbohydrates				
Glucose	166	0.72	0.72	0.67
Sucrose	325	0.48	0.46	0.52
Raffinose	480	0.38	0.36	0.43
Lactose	340	0.47	0.45	0.51 [a]
Maltose	340	0.47	0.45	0.47 [a]
Mannitol	185	0.67	0.67	0.66 [a]
Arabinose	148	0.77	0.78	0.77 [a]

Data for zwitterionic and neutral species were largely compiled by Hayduk and Laudie [11]. Data on carbohydrates partially[a] recomputed from 293 K data of Wilke [22] using Eq. (11).

6. Conclusions

The Generalized Maxwell–Stefan approach results in a good description of electric conductivity phenomena over a large range of aqueous electrolyte concentrations. The most important parameters required are infinite dilution diffusivities for the solute–solvent interaction. The necessary corrections for ionic transport at higher concentrations are the incorporation of electrostatic interaction of the ions and the viscosity increase of the solvent. The correlation by Wesselingh and Krishna [7] for the concentration dependent interaction of unlike ions, which is derived from transport properties of inorganic electrolytes, also works quite satisfactorily for organic ions. In this work, we did not investigate the interaction of like ions and the corresponding Maxwell–Stefan diffusion coefficients, but an analysis has been provided recently by Kraaijeveld and Wesselingh [13]. A modified Stokes–Einstein viscosity relation can account for the effects of the viscosity increase of the solvent at high electrolyte concentrations.

Therefore, conductivity measurements provide a rapid and reliable method to determine water–solute diffusivities of relatively complex organic electrolytes. As composition gradients do not occur, the technique is not hampered by gradients in thermodynamic non-ideality. An obvious disadvantage is of course its limitation to systems of electrolytes only.

Infinite dilution diffusion coefficients of polar solutes in water can be correlated by a modification of the Wilke and Chang relation, and with a somewhat smaller precision, with a modified Stokes–Einstein relation as proposed by Rutten [3]. This justifies the prediction of infinite dilution diffusivities from molecular structure only, using the group contribution method of LeBas.

7. Notation

c	Concentration, mol m^{-3}
D	Fickian diffusion coefficient, m^2 s^{-1}
$Đ$	Maxwell–Stefan diffusivity, m^2 s^{-1}
F	Faraday's constant 96 500, C mol^{-1}
I	Current density, A m^{-2}
I_x	Molar fraction based ionic strength
J	Molar flux mol m^{-2} s^{-1}
M	Molar mass
R	Gas constant 8.314, J mol^{-1} K^{-1}
R_i	Molecular radius, m
T	Temperature, K
x	Molar fraction
z	Spatial coordinate, m
z_i	Charge number of species i

7.1. Greek

γ	Activity coefficient
ϵ	Liquid fraction
κ	Conductivity, S m $\equiv$ A V^{-1} m^{-1}

λ Equivalent or molar conductance, S m^2 eq^{-1} or S m^2 mol^{-1}
ϕ Electric potential, V
χ Solvent association parameter in Eq. (4)

7.2. Subscripts

k,i,j Species
w Water
$+,-$ Cation, anion

Acknowledgements

One of the authors (LW) would like thank J.A. Wesselingh for the many discussions concerning mass transfer (and other not necessarily related items). Furthermore, the authors are grateful for the partial financial support of the Netherlands Organization for Scientific Research (N.W.O.) for this work. Gist-brocades is acknowledged for the free Penicillin G.

References

[1] R. Krishna, Diffusion in multicomponent electrolyte systems, *Chem. Eng. J.*, *35* (1987) 19–24.
[2] P. Vonk, Diffusion of large molecules in porous structures, *PhD Thesis*, Groningen University, The Netherlands, 1994.
[3] Ph.W.M. Rutten, Diffusion in liquids, *PhD Thesis*, Delft University of Technology, Delft, 1992.
[4] C.F. Wong and W. Hayduk, Correlations for prediction of molecular diffusivities in liquids at infinite dilution, *Can. J. Chem. Eng.*, *68* (1990) 849–859.
[5] J.S. Newman, *Electrochemical Systems*, Prentice-Hall International Series, Englewood Cliffs, NJ, 1991, 2nd edn.
[6] M.T. Tyn and T.W. Calus, Temperature and concentration dependence of mutual diffusion coefficients of some binary liquid systems, *J. Chem. Eng. Data*, *20* (1975) 310–316.
[7] J.A. Wesselingh and R. Krishna, *Mass Transfer*, Ellis Horwood, New York, 1990.
[8] R.C. Reid, J.M. Prausnitz and B.E. Poling, *The Properties of Gases and Liquids*, McGraw-Hill International Editions, Chemical Engineering Series, New York, 1988.
[9] A.D. Cadman, R. Fleming and R.H. Guy, Diffusion of lysozyme chloride in water and aqueous potassium chloride solutions, *Biophys. J.*, *37* (1981) 569–574.
[10] C.R. Wilke and P. Chang, Correlation of diffusion coefficients in dilute solutions, *AIChE J.*, *1* (2) (1955) 264–274.
[11] W. Hayduk and H. Laudie, Prediction of diffusion coefficients for nonelectrolytes in dilute aqueous solutions, *AIChE J.*, *20* (3) (1974) 611–615.
[12] Landolt–Börnstein, J. Bartels, P. ten Bruggencate, H. Hausen, K.H. Hellwege, Kl. Schäfer and E. Schmidt (eds.), Band II, 7, *Teil Elektrische Eigenschaften II*, Springer, Berlin, 1960.
[13] G. Kraaijeveld and J.A. Wesselingh, Negative Maxwell–Stefan diffusion coefficients, *Ind. Eng. Chem. Res.*, *32* (1993) 738–742.
[14] G.F. Versteeg and W.P.M. van Swaaij, Solubility and diffusivity of acid gases (CO_2, N_2O) in aqueous alkanolamine solutions, *J. Chem. Eng. Data*, *33* (1988) 29–34.
[15] E.D. Snijder, Metal hydrides as catalysts and hydrogen suppliers, Appendix 2, determination of diffusion coefficients with the Taylor dispersion method, *PhD Thesis*, University of Twente, 1992.
[16] A. Tsuji, E. Nakanishima, S. Hamano and T. Yamana, Physicochemical properties of amphoteric β-lactam antibiotics I: stability, solubility and dissolution behaviour of amino penicillins as a function of pH, *J. Pharm. Sci.*, *67* (8) (1978) 1059–1066.
[17] A. Tsuji, E. Nakanishima and T. Yamana, Physicochemical properties of amphoteric β-lactam antibiotics II: solubility and dissolution behaviour of aminocephalosporins as a function of pH, *J. Pharm. Sci.*, *68* (3) (1978) 308–311.
[18] R.C. Weast (ed.), *CRC Handbook of Chemistry and Physics*, CRC Press, Boca Raton, FL, 1982.
[19] W.J. Albery, A.R. Greenwood and R.F. Kibble, Diffusion coefficients of carboxylic acids, *Trans. Faraday Soc.*, *63* (1967) 360–368.
[20] J.M. Padfield and I.W. Kellaway, *J. Pharm. Pharmacol.*, *27* (1975) 348.
[21] H. Hikita, H. Ishikawa, T. Murakami and T. Ishii, Densities, viscosities and amine diffusivities of aqueous MIPA, DIPA, DGA and EDA solutions, *J. Chem. Eng. Jpn.*, *14* (5) (1981) 411–413.
[22] C.R. Wilke, Estimation of liquid diffusion coefficients, *Chem. Eng. Prog.*, *45* (3) (1949) 218–224.
[23] D. Crowfoot, C.W. Bunn, B.W. Rogers-Low and A. Turner-Jones, The X-ray crystallographic investigation of the structure of penicillin. In H.T. Clarke, J.R. Johnson and R. Robinson (eds.), *The Chemistry of Penicillin*, Princeton University Press, Princeton, NJ, 1949.
[24] E.H. Flynn, *Cephalosporins and Penicillins*, Academic Press, New York, 1972.
[25] M.T. Tyn and T.W. Gusek, Prediction of diffusion coefficients of proteins, *Biotechnol. Bioeng.*, *35* (1990) 327–338.